PROCEEDINGS, 47th Workshop on Geothermal Reservoir Engineering
Stanford University, Stanford, California, February 7-9, 2022
SGP-TR-223

Thermo-Poroelastic Effects on Permeability Change and Production Optimization in an Enhanced Geothermal Reservoir – Case Study of Deep Upper Jurassic Carbonates in the Bavarian Molasse Basin

[1]Ernesto Meneses Rioseco, [2]Michael Dussel, [1]Rinke Tegeler and [1,3]Inga S. Moeck

[1]Leibniz Institute for Applied Geophysics, Stilleweg 2, 30655 Hannover, Germany

[2]Ruhr-Universität Bochum, Universitätsstraße 150, 44801 Bochum, Germany

[3]Georg-August-Universität Göttingen, Wilhelmsplatz 1, 37073 Göttingen, Germany

Ernesto.MenesesRioseco@leibniz-liag.de

Keywords: 3-D geothermal reservoir modelling, numerical simulation, coupled thermo-hydro-mechanical reservoir processes, naturally fractured reservoir, EGS, permeability variations, production optimization, multi-stage hydraulic treatments, open-hole stimulation completion, proppants placement, North Alpine Foreland Basin

ABSTRACT

Optimal stimulation design and long-term sustainable management of enhanced geothermal systems (EGS) can benefit from numerical modelling and simulation of coupled fracture deformation, fluid flow and heat transport. The mechanical response of the fracture-matrix system influences reservoir permeability variations due to cold fluid injection and production processes. We adopt a multidisciplinary approach within the framework of the joint research project ZoKrateS, which comprises extensive completion and stimulation operations to enhance the productivity of a petrothermal reservoir in ultra-deep Upper Jurassic carbonates of the Bavarian Molasse Basin. We develop a 3-D, fully coupled thermo-hydro-mechanical reservoir model to simulate the spatiotemporal thermo-poroelastic response of a stress-sensitive fracture-controlled reservoir. For the 3-D static geomodelling and dynamic finite-element analyses, we use SKUA-GOCAD™ and COMSOL Multiphysics®, respectively. The numerical model combines non-isothermal compressible single-phase fluid flow in fractured porous rock and heat transfer with an optimization algorithm for the geothermal energy production task. We consider a nonlinear fracture deformation model to investigate the role of coupled processes on fracture deformation, stress redistributions and production performance. In particular, poromechanical effects of the reservoir are assumed to play an important role based on previous observations made during drilling operations and hydraulic tests, which suggest that reservoir matrix deforms and fractures close up during increasing effective stress, leading to variations in fracture permeability and production performance. We employ structural interpretations of a 3D seismic survey in the license field Wolfratshausen ca. 40 km south of Munich, logging, mud losses, zones of joint calcites and well tests in the 5700 m MD long borehole GEN-1ST-A1 near Geretsried to accurately implement hydraulically active faults and fractures in a 3D reservoir model. We model the present-day, undisturbed 3-D temperature distribution taking into consideration the regional temperature gradient, temperatures measured in the borehole and thermo-physical parameters measured in former, local geothermal research projects. In addition, we develop a 3-D geomechanical model, which considers a most likely strike–slip stress regime in the 4.5 km deep reservoir by choosing adequate boundary conditions in line with the governing stress field and geomechanical data compiled in the previous project Dolomitkluft. We further constrain the geomechanical model by taking into account pressures derived from formation integrity tests (FIT) and stress-limiting conditions. Concerning geothermal energy production optimization, we analyze simulation results to draw conclusions on the controls of the optimal placement of a second well under different cold fluid injection or production strategies. Based on our numerical experiments, we conclude on the role of coupled thermo-hydro-mechanical reservoir processes on fracture deformation, permeability variations and heat transport. We focus on the implications that these coupled reservoir processes have for a long-term sustainable utilization of geothermal energy in a doublet operational scheme.

1. INTRODUCTION

Deep and low-permeability hot rocks, where a pre-existing fracture network provides the fluid flow and heat exchanging capabilities, constitute an important but challenging geothermal resource to develop. Harnessing the geothermal energy from such geothermal resources, which are naturally not productive enough for an economic direct use, requires a profound understanding of the coupled thermo-hydro-mechanical behavior of the geothermal reservoir under different exploitation strategies. In addition, from the technical implementation viewpoint, efficiently developing the geothermal energy hosted in such tight and hot rocks requires considerable efforts for the reservoir treatment design and the implementation of high-end completion and reservoir stimulation technologies to enhance the long-term permeability of the reservoir and hence the productivity.

With the purpose of creating an enhanced/engineered geothermal system (EGS) in a structurally controlled petrothermal reservoir and to show the effectiveness of proppants, which were not yet used in the deep geothermal sector, several zones of a naturally fractured low-permeability carbonate reservoir were successfully stimulated in the framework of the demonstration and pilot joint research project ZoKrateS. This project set out at the beginning of 2020 with different partners from the research and private sectors to target low-porosity, low-permeability Upper Jurassic (Malm) carbonates in deeper sections of the North Alpine Foreland Basin (NAFB), ca. 40 km south of the capital city of Munich (Germany). The ZoKrateS project team involves academic and research institutions such as the Ruhr University Bochum (lead) and the Leibniz Institute for Applied Geophysics (LIAG) as well as companies like ENEX Geothermieprojekt Geretsried

Nord GmbH & Co. KG (drilling site owner, operator), Geothermie Neubrandenburg GmbH (GTN) and G.E.O.S. Ingenieurgesellschaft mbH. Operative works were planned and supervised by KEMCO GmbH (Drilling Management Consulting) and executed by Daldrup & Söhne AG and Schlumberger.

In this work, we focus on the development of 3-D numerical models to study the long-term thermoporoelastic behavior of the reservoir resulting from envisaged cold fluid injection and production profiles. To be able to examine the long-term thermoporoelastic impact that geothermal doublet operational profiles have on the overall performance and sustainability of the reservoir development, numerical simulations incorporating theoretical, fictitious geothermal wells are conducted. This is intended to assess the controls on the optimal placement of a second geothermal well in addition to the already drilled sidetrack GEN-1ST-A1 (see Fig. 1 and text below). The 3-D model is based on a comprehensive data analysis, partly gathered in the preceding project Dolomitkluft [Wolfgramm et al. (2019), Thuro et al. (2019), Moeck et al. (2019), Kahnt et al. (2019), Dussel et al. (2018) & (2019)], and the recent interpretation of the 3-D seismic survey [Shipilin et al. (2020)] in the license field Wolfratshausen, in the southern South German Molasse Basin, which is part of the NAFB.

After two failed attempts to harness geothermal energy from the deep Upper Jurassic reservoir – the wellbore Geretsried GEN-1 in 2013, which targeted supposedly productive massive carbonate facies and the sidetrack GEN-1ST-A1 in 2017, which targeted a crosscutting zone of syn- and antithetic faults of the Gartenberg fault zone [Dussel et al. (2018), Shipilin et al. (2020)] -, the reservoir in question was further investigated for the development of an enhanced petrothermal reservoir. The observation in 2017 that the injectivity in the sidetrack was higher than the productivity (transmissivity for the entire fault zone of $T=6.5*10^{-5}$ m^2/s) suggests that thermoporoelastic effects in naturally fractured limestones and dolostones may play a critical role.

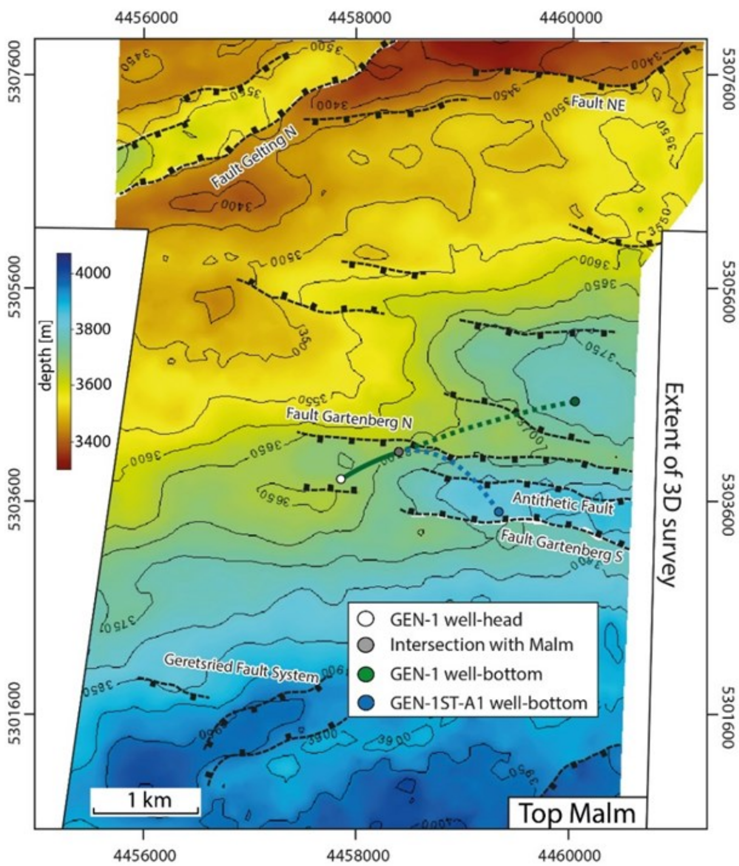

Figure 1: Plan view of the Top Malm (top reservoir) displaying the projection of the well paths related to GEN-1 and the sidetrack GEN-1ST-A1. Note the Gartenberg fault system (Gartenberg graben) interpreted by Shipilin et al. (2020) in the middle, which is crossed by the sidetrack GEN-1ST-A1 depicted in blue with a dotted line. The drilling site is located in the Bavarian part of the North Alpine Foreland Basin [e.g. Dussel et al. (2018)], around 40 km south of the capital city of Munich (Germany). Notice the gently dipping strata.

In preparation for the stimulation job in autumn 2021, a microseismic monitoring network with 5 stations was installed, together with a particular sensitive alerting scheme, which might be exemplary for future stimulation jobs in the geothermal industry. Recent borehole measurements in August 2021, which consisted, among others, of formation microimaging (FMI) and Full Waveform Sonic revealed in detail the effects of the acidizing jobs in 2017 and hydraulic active structures [Schlumberger (2021)] at the Gartenberg North fault. These findings were especially useful to optimize the hitherto existing stimulation plan. Based on these findings, a new, innovative and detailed completion scheme for the geothermal industry could be realized. While hydraulic treatment with in total injected ca. 330 t of proppants in three zones only required a slight pressure increase, this injection pressure was well below the fracture gradient (FG). A lower than expected wellhead pressure of approx. 320 bar (see Sect. 3) was necessary to inject proppants into the in 2017 [Dussel et al. (2018)] acidized natural fracture system. Preliminary analysis of a short-term hydraulic test suggests an enhancement of the hydraulically active groundwater pathways and indicates the effectiveness of the hydraulic treatment.

2. RESERVOIR GEOLOGY AND DATASET

Deep Upper Jurassic carbonates drilled by the sidetrack GEN-1ST-A1 showed to be highly fractured [Moeck et al. (2019), Thuro et al. (2019), Stockinger (2021)]. The geothermal reservoir at a depth of ca. 4.5 km consists mainly of ca. 70 m thick Purbeckian dolomites and ca. 580 m thick Upper Jurassic micritic carbonates and dolomites. Regional strata (see Fig. 1) is slightly dipping towards the south. The most prominent tectonic structure in Upper Jurassic limestones and dolostones in the study area constitutes the E-W striking Gartenberg fault zone [Shipilin et al. (2020)].

Table 1: Simplified stratigraphic chart and model layers.

Stratigraphic/geotectonic unit	Lithology	Thickness [m]	Model layer
Quaternary	Gravel	70[3]	Not considered
Tertiary	Predominantly clay marl, marl, sandstone; **Base**: Lithothamnion limestone	4,120[3]	Overlying section[2]
Cretaceous (without Purbeckian unit)	Clay marl, marl lime, limestone	170[3]	Overlying section[2]
Purbeckian section	Dolomite	70[5,6]	Reservoir
Upper Jurassic (Malm)	Mainly micritic limestone, dolomite	580[1,3]	Reservoir
Dogger	Marly limestone, sandstone	30[4]	Underlying stratum
Moldanubicum (basement)	Granite, gneiss		Underlying stratum

(1) Based on regional data and supported by 3-D seismic interpretation, base Malm not drilled

(2) Only ca. 1 km considered due to model setup

(3) Straubinger & Gahr (2018); (4) Bachmann & Müller (1991); (5) Wolfgramm et al. (2019); (6) Thuro et al. (2019)

2.1 Well Inflow Zones

In the following, we summarize the main findings concerning the identification and delineation of hydraulic active zones in the crosscutting of the Gartenberg graben. As mentioned earlier, the exploration concept followed to drill the sidetrack GEN-1ST-A1 involved a highly fractured damage zone of the Gartenberg fault system. Roughly, limestones and dolostones are well known in the literature to be more brittle than sandstones. In this context, during an intensive faulting activity in the Ruppelian time, the Upper Jurassic carbonates most probably experienced extensive fracturing within the damage zone of the crossing conjugate normal faults. However, constraining the hydraulic activity of such fault and fracture system is a challenging task.

At the drilling site, the carbonate reservoir was drilled at 4.4 to 4.8 km depth (TVD) into the Gartenberg Graben (see Fig. 1 and 7). We use multidisciplinary and multiscale data collected in the sidetrack GEN-1ST-A1 [Wolfgramm et al. (2019), Moeck et al. (2019), and Thuro et al. (2019)], to delineate potential hydraulically active zones. Based on the interpretation of the 3-D seismic survey (Fig. 1), mud losses, borehole measurements, laboratory measurements on cores and joint calcites in cutting samples, groundwater flow is fundamentally controlled by fractures and not by low matrix porosities in the range of 1 to 2 % [Thuro et al. (2019)] and can therefore be interpreted as potential inflow zones [Dussel et al. (2019), Wolfgramm et al. (2019)]. Inferred from an intensive and integrative data evaluation [e.g. Meneses Rioseco et al. (2022)], potential inflow zones were identified and gave preliminary information for choosing stimulation zones. To show some examples, data from a Full Waveform Sonic Log and the interpretation of an Image Log in 2017 is displayed in Fig. 2. In

2021 additional well logs were run, which specified more precisely the permeability structure of the Gartenberg fault system and led to a site-specific optimized stimulation strategy [see Sect. 3 and Schlumberger (2021)].

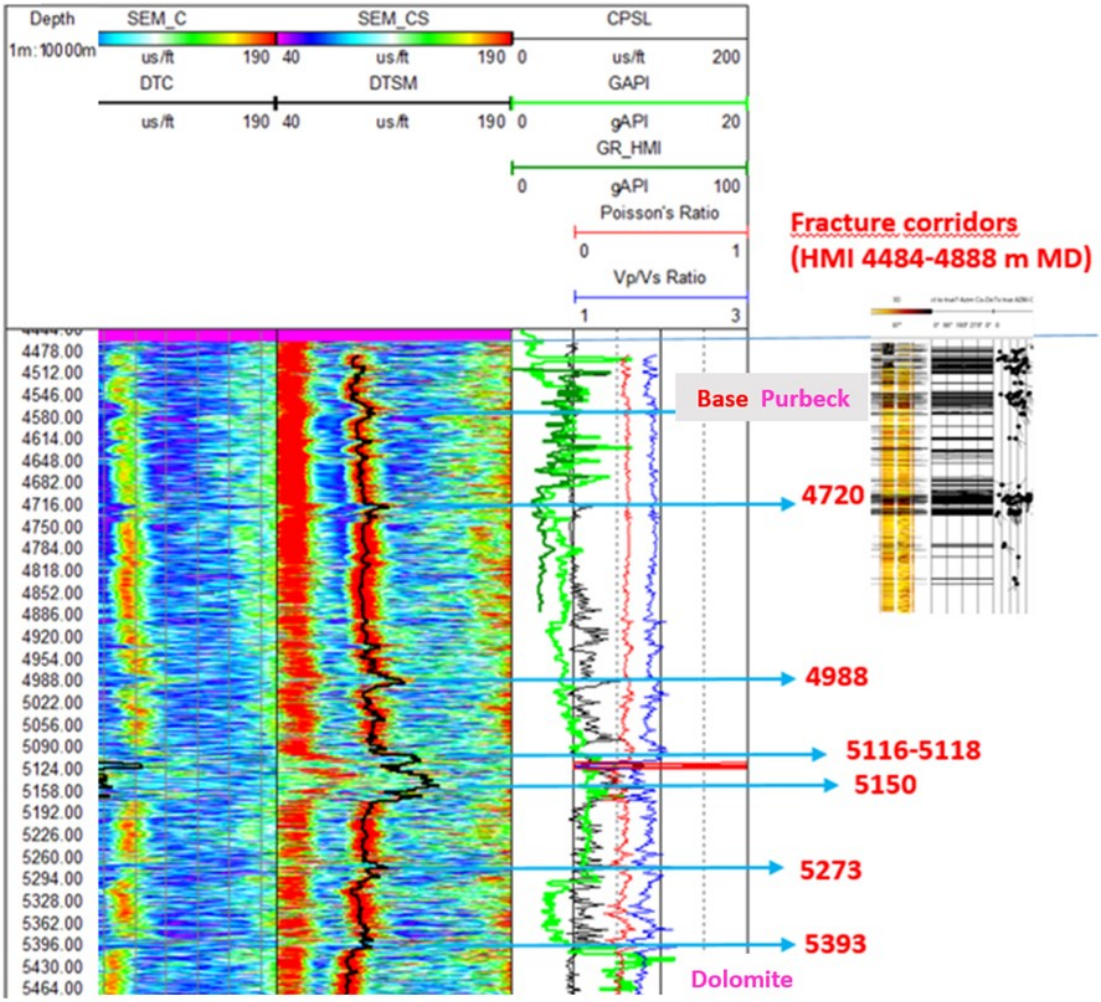

Figure 2: Logging corresponding to the sidetrack GEN-1ST-A1 (2017). Compressional and shear wave travel-times from Full Waveform Sonic (FWS) with highest travel times coinciding with the zone of total mud loss (5116 – 5118 m mD), which corresponds to the crosscutting of the Gartenberg North fault (see Fig. 1), as well as high fracture density (right column, indicated by black lines) from Image Logging (HMI) were used together with further Logs [see Meneses Rioseco et al. (2022), Dussel et al. (2019)] for delineating potential inflow zones.

3. COMPLETION & STIMULATION DESIGN

The well GEN-1ST-A1 was drilled in 2017 as a sidetrack from the J-shaped pilot hole GEN-1 to a TD of 5700 mMD (4736 mTVD). The basis of well design consisted of a 32” conductor, 20” surface CSG, 13-5/8” intermediate CSG, 9-5/8” intermediate liner and a 7” production liner to 4485 mMD. The 6” reservoir section was drilled horizontally with up to 85° inclination on a length of approx. 1200 m. The well penetrated the Gartenberg fault zone, encountering a complex network of natural fractures with up to 29 FF/m. After reaching TD, the well was completed barefoot and an acid squeeze job with more than 350 m³ 15% HCl has been performed on the open-hole. As the well test results were below expectations for a hydrothermal development concept, the well was temporarily abandoned.

During the project ZoKrateS in 2021 the 6“ reservoir section has been completed open-hole with a 4-1/2“ multistage stimulation liner (Fig. 3) and a 5-1/2“ TBG to surface. Key element of the completion design were CT-activated sliding sleeves to provide precise control of the fracture placement. Zonal isolation between the stages was established by using a combination of mechanical and swellable OH packer. Packer placement and definition of stimulation zones were strongly influenced by the wellbore caliper, which has been affected by the previous acid job in 2017. Nevertheless, four stimulation stages between 5700 - 4564 mMD could be isolated with OH packers (Fig. 3). The stimulation ports were placed in areas with highest natural fracture density. Once the completion was installed, the sleeves were manipulated via coiled tubing shifting tool allowing a selective hydraulic stimulation of each stage one after another. This design also gave the benefit to evaluate the performance of each individual stage during the well test phase. The hydraulic stimulation was pumped through the annulus between 4-1/2“ liner and 2-7/8“ coiled tubing. Key challenges for the completion design were comparably high temperatures up to 163°C and low reservoir salinity. The downhole conditions were affecting the reliability of rubber seals and the function of certain completion tools. The initial design concept using a ball-activated sleeve completion has been replaced by a CT-activated system at an early stage due to major uncertainties for final pad volumes. Completion & stimulation via cemented liner and plug & perforate technology – as widely used in the shale industry - was rejected due to risk of severe skin damage in the underbalanced, naturally fractured reservoir section. Three out of four stages could be successfully stimulated. The last sliding sleeve giving access to stage #4 could not be opened due to technical issues.

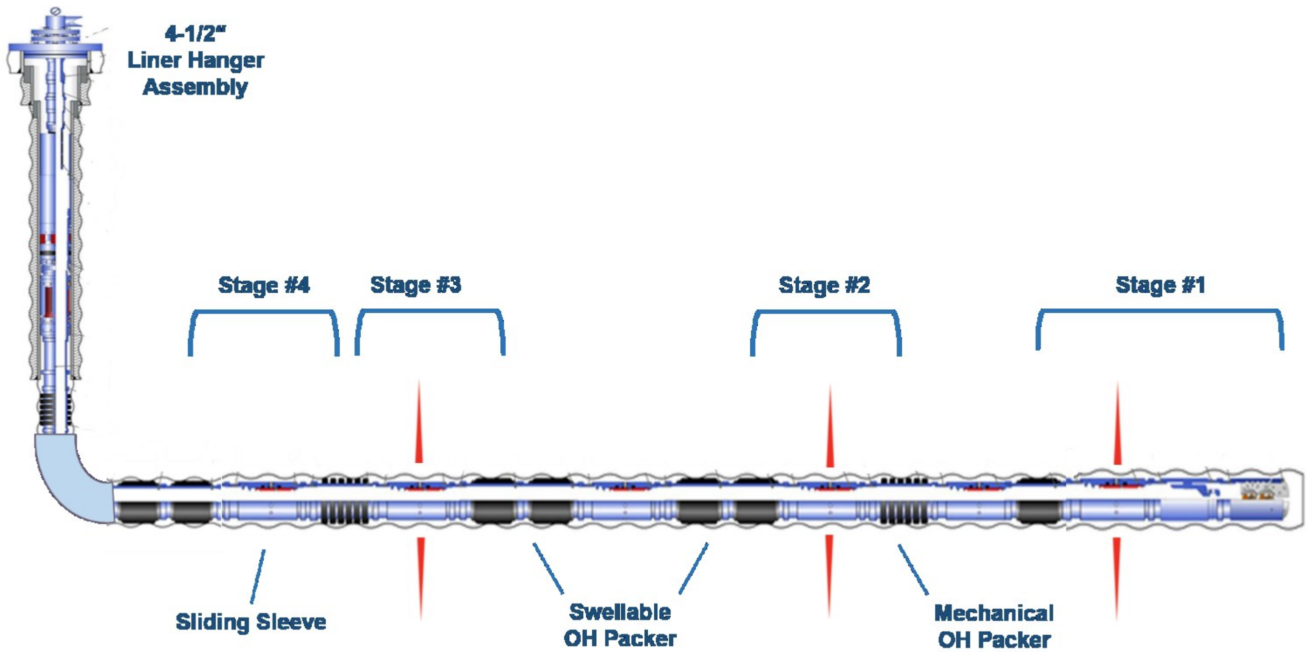

Figure 3: Completion schematic of the GEN-1ST-A1 multistage stimulation completion design.

The hydraulic stimulation of GEN-1ST-A1 was designed as a multistage gel treatment with fluid volumes in the order of 400 – 600 m³ per stage. As for the stimulation fluid Schlumberger's ThermaFRAC™ product, which is optimized for high temperature applications, has been used. Beside the temperature stability of gel and additives, the fluid design had to fulfill German environmental requirements. To keep the fractures open after bleed-down, there has been used a blend of 30/50 and 20/40 high strength ceramic proppant (Fig. 4). For better proppant transport, fibers were added to the crosslinked fluid. During stimulation of the three stages, a total amount of approx. 330 t of proppants has been placed in the natural fracture network.

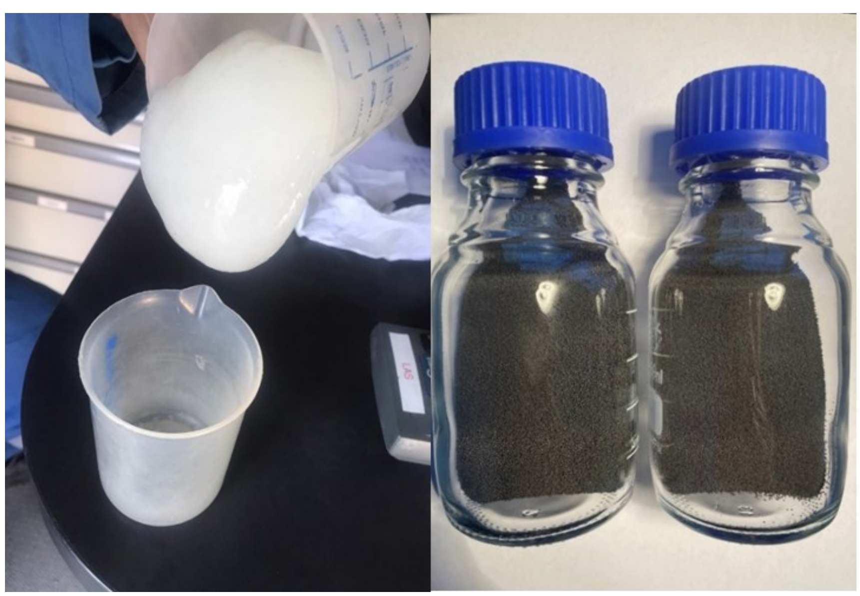

Figure 4: Crosslinked stimulation fluid at 70 °C (left) and high strength ceramic proppants (right).

The stimulation equipment incorporated 5x HP stimulation pumps, polymer- & proppant blenders and 3x 190 m³ pillow tanks for mixing water storage (Fig 5). Furthermore, a coiled tubing unit became necessary for shifting the sleeves and as a backup for clean-out runs between stimulation of the stages. The stimulation fluid was mixed on-the-fly during the treatment with additives concentration automatically being adjusted to pad and slurry requirements. The pump rates were limited to 5.0 m³/min. Surface treatment pressures were lower than expected and did not exceed 320 bars. During the whole stimulation treatment, a stationary seismic monitoring network was in place. After stimulation job, the well was put on flowback for a period of 3 days. Returns were routed to an O&G well test package with a cyclone desander and 3-Phase separator to remove residues of proppant and traces of hydrocarbons. After bleed-down, the well performance was tested via airlift using the drillstring of the rig.

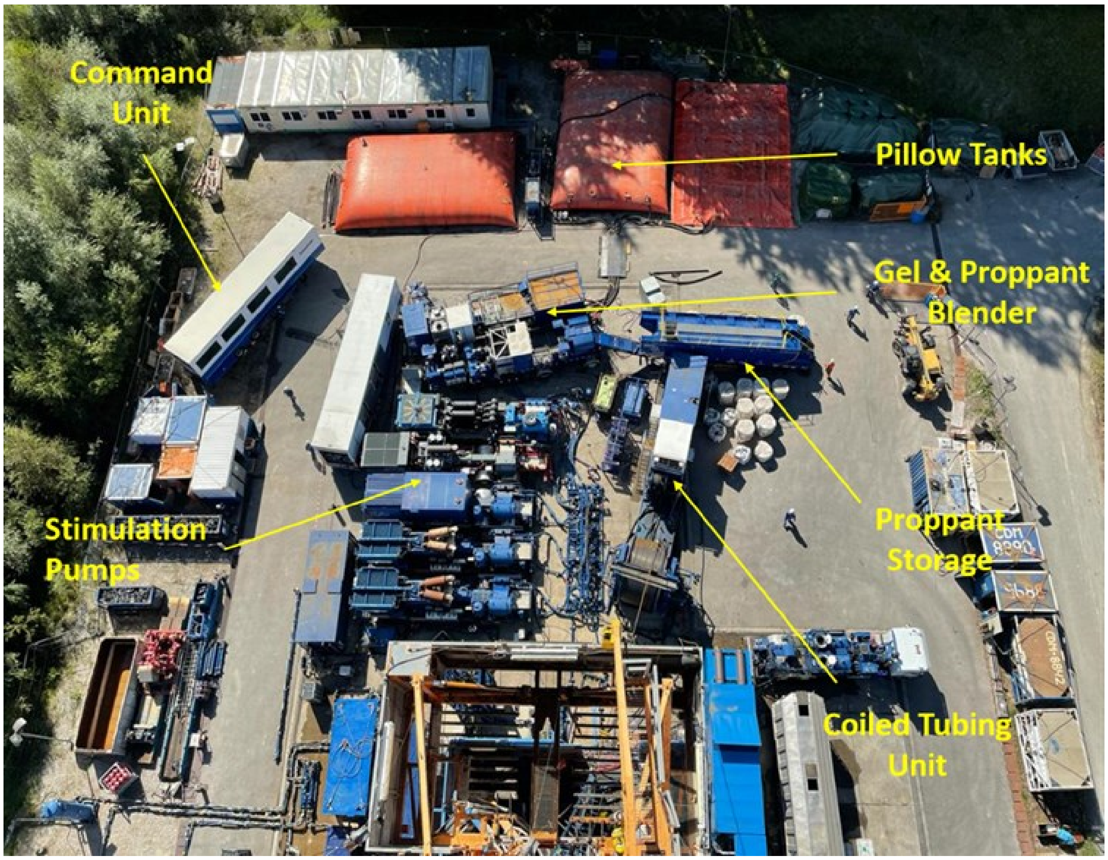

Figure 5: Surface stimulation equipment.

4. TRANSIENT THEORETICAL FORMULATION OF THERMOPOROELASTICITY

First presented by Biot (1941) and further developed by Rice and Cleary (1976), the 3-D isothermal theory of poroelasticity describes the mechanics of deformation of fluid saturated porous media. Thermoporoelasticity additionally considers induced thermal stresses and deformation. The effect on temperature changes on the poroelastic behavior of the porous rock-fluid system can be accounted for by using the following constitutive equations introduced by McTigue (1986) and documented in detail by Wang (2000):

$$\sigma_{ij} = 2G\varepsilon_{ij} + \delta_{ij}(\lambda_u\varepsilon_v - \alpha M\zeta) + \delta_{ij}K_d\beta_s\Delta T \quad (1)$$

$$p = M(\zeta - \alpha\varepsilon_v + \beta_m\Delta T). \quad (2)$$

Here, σ_{ij} and ε_{ij} stand for the components of the total stress and strain tensors, respectively. G and λ_u express the shear modulus and undrained Lamé's first parameter, ε_v denotes the volumetric strain, α represents the Biot coefficient, M is the Biot modules and ζ indicates the increment of fluid content. K_d represents the drained bulk modulus, β_s is the linear thermal expansion coefficient of the solid material and ΔT indicates the temperature change. In equation (2), p denotes the pore pressure and β_m expresses the changes in fluid mass content at constant confining pressure and pore pressure.

When combining these constitutive equations with the equilibrium and conservation equations, the governing equations describing the transient thermoporoelastic behavior of porous rock saturated with fluid circulating or trapped in the porous space [McTigue (1986); Biot (1962)]:

$$G\nabla^2\boldsymbol{u} + (\lambda_u + G)\nabla(\nabla\cdot\boldsymbol{u}) + \rho_b\boldsymbol{g} = \alpha\nabla p + K_d\beta_s\nabla T \quad (3)$$

$$S_v\frac{\partial p}{\partial t} + \nabla\cdot\left[-\frac{k}{\eta}(\nabla p + \rho_f g z)\right] = -\alpha\frac{\partial \varepsilon_v}{\partial t} + \beta_m\frac{\partial T}{\partial t}, \quad (4)$$

where the nabla symbol ∇ represents the gradient when applied to a scalar field and the divergence when applied to a vector field. ρ_b and ρ_f express the density of the bulk material and fluid, respectively. The permeability and fluid viscosity are denoted by k and η, the gravitational acceleration vector is $\boldsymbol{g}$. The storage coefficient S_v is given by the inverse of the Biot modulus M, which is in turn defined assuming invariable volumetric strain and temperature as follow:

$$S_v = \frac{1}{M} = \frac{\phi}{K_f} + \frac{(\alpha-\phi)(1-\alpha)}{K_d}, \quad (5)$$

in which ϕ represents the porosity and K_f is the fluid bulk modulus. The application of the thermoporoelasticity theory in COMSOL Multiphysics® is explained at great length in the Structural Mechanics Module User's Guide and COMSOL Mutiphysics® manual.

4.1 Heat Transport in Porous Fractured Media

Heat transfer involves fundamentally diffusion and advection processes and is formulated based on the energy conservation. A detailed description can be found for instance in Blank et al. 2021 and the Heat Transfer Module User's Guide of COMSOL Multiphysics®. In saturated porous media, the heat transport equation as implemented in COMSOL Multiphysics® reads as:

$$(\rho C_p)_{eff}\frac{\partial T}{\partial t} + \nabla\cdot(\rho C_p\boldsymbol{u}T) + \nabla\cdot\boldsymbol{q} = Q_h. \quad (6)$$

Here, C_p refers to the fluid capacity at constant pressure, whereas $(\rho C_p)_{eff}$ stands for the effective volumetric heat capacity at a constant pressure. In equation (6), $\boldsymbol{u}$ represents the Darcy velocity. The diffusion part of the equation is given by the conductive heat flux $\boldsymbol{q} = -\lambda\nabla T$, where λ denotes the effective thermal conductivity. With the term Q_h on the right hand side, we take into account the presence of heat sources or sinks. As explained previously, fracture fluid flow is governed in this work by the cubic law. We compute the heat transport in fractures in a similar way as in equation (6) for the porous media. However, a slight modification of equation (6) is made to account for the fracture permeability related to the fracture hydraulic aperture (parameter b):

$$b(\rho C_p)_{eff}\frac{\partial T}{\partial t} + \nabla_t\cdot(b\rho C_p\boldsymbol{u}_t T) + \nabla_t\cdot\boldsymbol{q_{fr}} = bQ_h, \quad (7)$$

with the subscript *t* denoting the tangential derivative. Besides, $\boldsymbol{u_t} = k/\eta\ (\nabla_t p)$ describes the tangential Darcy velocity and $\boldsymbol{q_{fr}} = -b\lambda_{fr}\nabla_t T$ characterizes heat conduction in the fracture domain. $(\rho C_p)_{eff}$ is computed only within the fracture-fluid volume and λ_{fr} refers to the thermal conductivity of the fracture. The fracture hydraulic aperture is a key control on the rate of heat transfer in the fracture-matrix system. Parallel to the fracture surface, heat advection dominates for hydraulically conductive fractures, whereas heat conduction constitutes the prevailing mechanism perpendicular to the fracture surfaces, in particular for low-porosity and low-permeability reservoirs.

4.2 Physical Nonlinearities Implemented in the Numerical Model

We implement in this work physical nonlinearities such as temperature- and pressure-dependent density and viscosity according to Diersch 2014 and values reported in international steam tables [Kretzschmar & Wagner (2008)]. Fig. 6 (left) graphically shows the function adopted for the pressure- and temperature-dependent density. Besides, we integrate in the cubic law used for fracture fluid flow (Witherspoon et al. 1980) a highly nonlinear fracture aperture dependent on the compressive normal stress resolved on the respective fracture surfaces (Barton-Bandis model after Barton & Bandis (2017) and references therein). This is implemented to account for the fracture permeability variations in tight rock joints resulting from the injection and production schemes considered in this study.

Based on laboratory experiments, a hyperbolic relationship between fracture normal closure δ_n and normal compressive stress σ_n has been proposed by Goodman (1976), see eq. (8). This hyperbolic model is defined by two further constraints, which are the fracture initial normal stiffness K_{n0} at relatively low stresses and a maximum fracture closure δ_{max} at comparatively high stress:

$$\sigma_n = \frac{K_{n0}\delta_n}{(1-\delta_n/\delta_{max})} \quad . \quad (8)$$

Fundamentally, this model describes the observation that an increase in compressive normal stress results in a fracture deformation normal to its walls and eventual closure of the fracture. Barton & Bandis (2017) summarized a series of laboratory experiments conducted by them in the 80s and 90s that revealed that rock type and joint type plays a critical role in the fracture closure behavior. Ultimately, the authors defined the normal stiffness of the fracture K_n as the total derivative of the hyperbolic function mentioned before (eq. 8) with respect to the normal displacement δ_n (see also Fig. 6, right):

$$K_n = \frac{d\sigma_n}{d\delta_n} = \frac{K_{n0}}{(1-\delta_n/\delta_{max})^2} \quad . \quad (9)$$

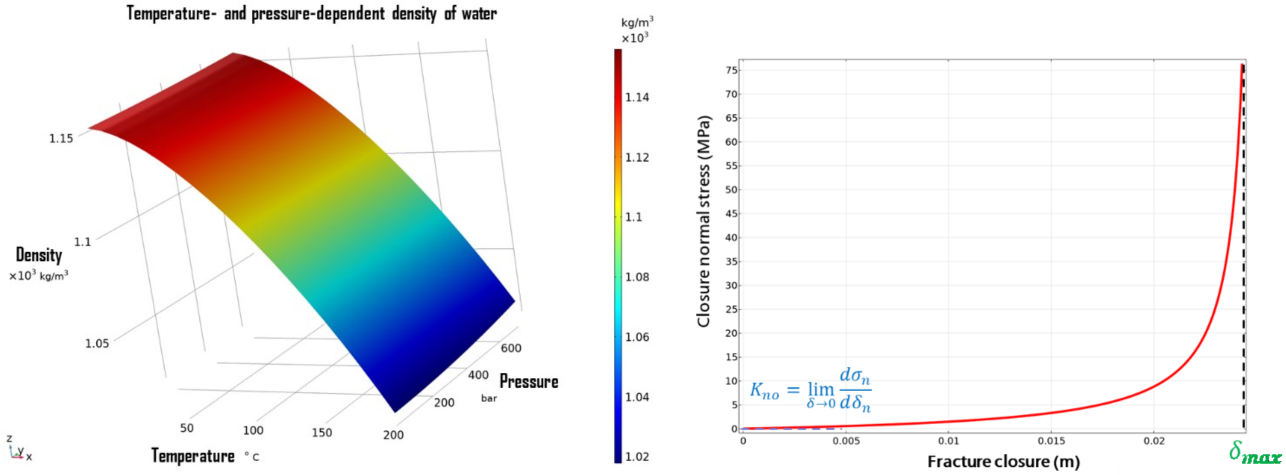

Figure 6: Left: Temperature- and pressure-dependent density function implemented in the model. International steam tables have been used after Kretzschmar & Wagner (2008) and widely known relationships for the equations of state for water reported in Diersch 2014 have been employed. Right: Highly nonlinear behavior of fracture deformation under compressive normal stress, which has been implemented in the numerical model. Note that K_{no} denotes the initial fracture normal stiffness at lower normal stresses. δ_{max} is a maximum fracture closure assumed at high stresses.

5. MODEL SETUP

We build a 3-D geothermal reservoir model by incorporating multi-scale geophysical, geological and drilling operation data collected in the sidetrack GEN-1ST-A1 [Shipilin et al. (2020), Wolfgramm et al. (2019), Kahnt et al. (2019), Thuro et al. (2019), Moeck et al. (2019), and Straubinger & Gahr (2018)]. For the purpose of finite-element dynamic simulation, we convert the structural and stratigraphic model, developed by Shipilin et al. (2020) from seismic interpretation, into a reservoir model adequate for finite-element meshing. Fault and stratigraphic horizons modelling in our study consisted in enhancing with SKUA-GOCAD™ the connectivity between faults, the fault intersections and the fault-horizon intersections to create a watertight structural model, where the intersections between all faults and horizons are properly defined. Aiming for a watertight model is crucial, in particular for the construction of the 3-D grid in the subsequent step of the modelling workflow. In addition, the open-hole section of the sidetrack GEN-1ST-A1 is integrated in the reservoir modelling domain, which crosses the Gartenberg fault and fracture system, see Fig. 7. Further details can be read in Meneses Rioseco et al. 2022.

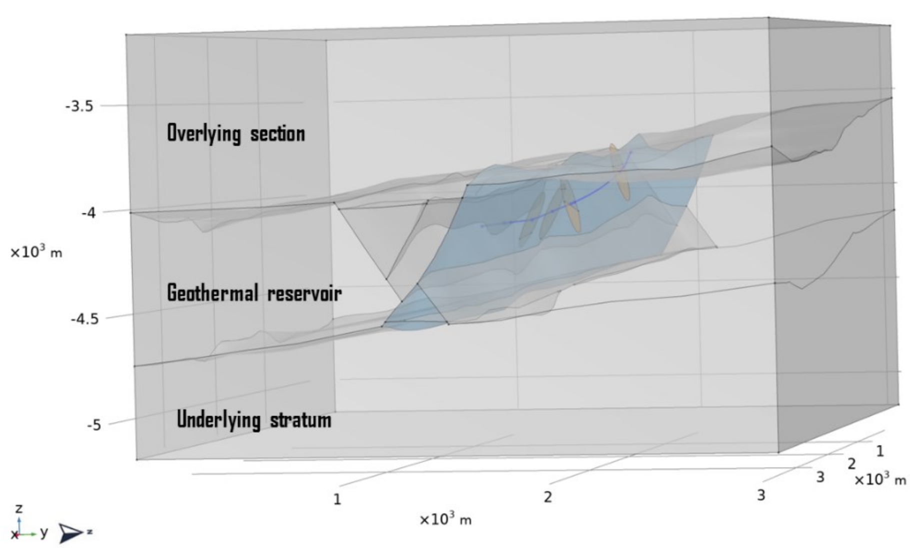

Figure 7: 3-D subsurface model initially setup for preliminary studies and visualization purposes. Three main layers have been implemented in the model. The middle layer shows the Upper Jurassic carbonates, target of geothermal exploration in the North Alpine Foreland Basin. The focus of this study constitutes the Gartenberg fault and fracture system, displayed in the middle of the modelling domain, where recent data has been collected in the sidetrack GEN-1ST-A1. Note the Gartenberg North fault depicted in light blue, where an inflow zone has been clearly detected, four additional penny-shaped fractures shown in orange, and the open-hole section of the sidetrack GEN-1ST-A1 integrated in the model as bold line in dark blue.

Using the finite-element software COMSOL Multiphysics®, we carry out several mesh convergence studies. Besides, extensive preliminary studies concerning the influence of spatial and temporal discretization were conducted. Mesh refinement operations in regions of high hydraulic gradients and sharp contrasts in thermal and mechanical properties have been conducted, see Fig. 8. The minimum and maximum element sizes defined are 1.51 m and 151 m, respectively. The adopted parametrization of the mesh led to a total number of tetrahedral elements equal to 1,620,826.

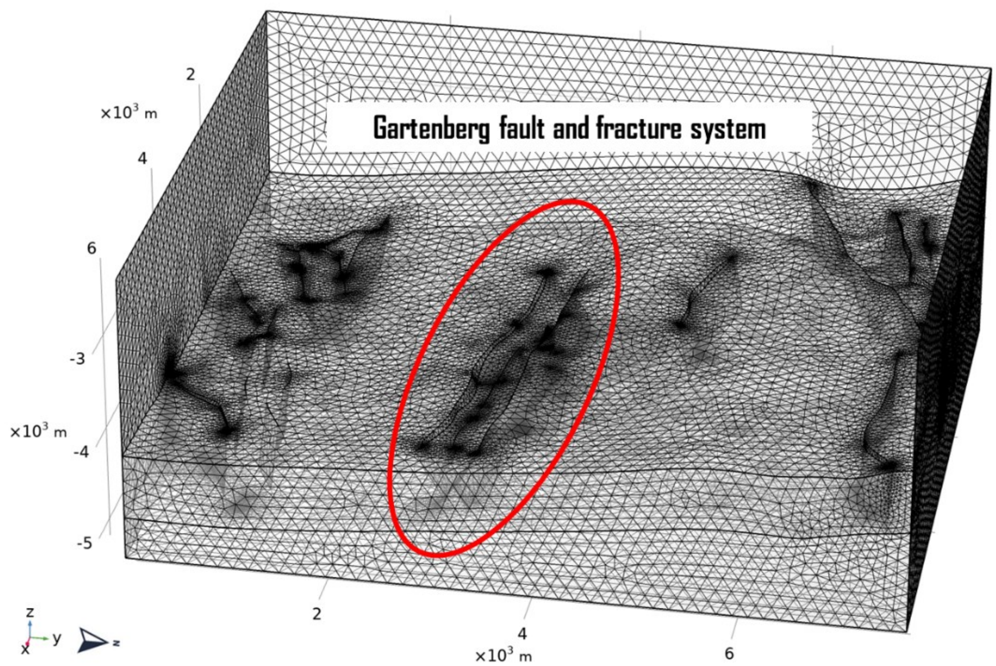

Figure 8: 3-D finite-element, unstructured tetrahedral volume mesh refined at high-gradient structures and in the region of most interest in the model (center of the modelling domain displaying the Gartenberg fault and fracture system indicated with a red circle). Note that the y-axis denotes the North direction.

4.1 Initial and Boundary Conditions - Parametrization

Hydraulic tests are the most meaningful and encompassing methods to derive hydraulic parameters and fluid behavior at reservoir-scale [Bourdet (2002)]. Based on a production test carried out in 2017 within the preceding project Dolomitkluft [Wolfgramm et. al. (2019), Kahnt et al. (2019)], pressure transient analyses and in particular curve fitting operations have been conducted to derive the hydraulic parameters of the matrix-fracture system. Especially the hydraulic fracture aperture plays a critical role in a fracture-controlled reservoir. Hence, parameter sensitivity studies using different optimization algorithms for the curve fitting procedure of the built-up phase of the production test have been undertaken (see Fig. 9).

To specify the solution for the one-phase transient groundwater flow equation in confined and saturated reservoir conditions, derived from the momentum and mass conservation equations, it is required to prescribe initial and boundary conditions along all boundaries of the model. A prescribed constant hydraulic head (Dirichlet condition) according to measurements conducted has been set along the lateral boundaries of the model. A no-flow boundary condition (Neumann condition) has been adopted for the top and base of the model and constant fluid flux (Neumann condition) has been defined to impose inflow and outflow rate at wellbores. For the heat balance equations (6) and (7), a prescribed temperature gradient of $\sim 30.5\,℃/km$ (Dirichlet condition), derived from temperature log measurements conducted in the sidetrack GEN-1ST-A1 and thermal insulation (Neumann condition) at the top and base of the model has been imposed. Employing the above boundary conditions, unperturbed initial pressure and temperature conditions are obtained by stationary simulation. This initial temperature distribution is perturbed by the injection of cold water ($\sim 60\,℃$) at different injection rates into the reservoir through the highly deviated open-hole section of the sidetrack GEN-1ST-A1.

The geomechanical initial and boundary conditions of the model are illustrated in Fig. 10. These initial and boundary conditions are imposed to implement a strike-slip stress regime in the reservoir, which is the estimated present-day stress state in the reservoir, e.g. Stockinger (2021). The maximum horizontal stress has been set in the North-South direction, roughly perpendicular to the Alpine Thrust Front, according to Reinecker et al. (2010) and Ziegler et al. (2016). Elastic material parameters for the reservoir are set according to values reported in Stockinger (2021). We populate the underlying and overriding strata with elastic parameters discussed in Ziegler et al. (2016) and references therein.

As explained above, beside the adopted initial and boundary conditions, the parametrization has been performed by history matching observed flied data (hydraulic tests, temperature log) with the reservoir model and material properties gathered in the sidetrack GEN-1ST-A1 in the preceding project Dolomitkluft [Wolfgramm et al. (2019), Kahnt et al. (2019), Moeck et al. (2019), Thuro et al. (2019), Stockinger (2021)]. The interested reader is encouraged to read Meneses Rioseco et al. (2022) for a more detailed description of the parametrization of the model.

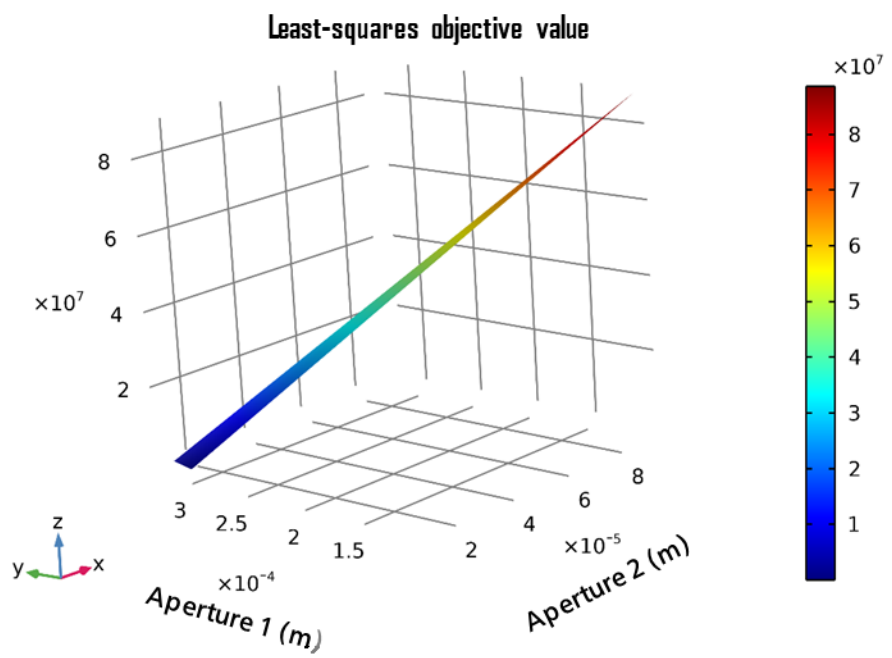

Figure 9: Least-squares objective values showing the minimum value of the minimized objective function obtained for the curve fitting procedure of the build-up phase of the production test conducted in 2017 in the sidetrack GEN-1ST-A1. Note that different combinations of hydraulic fracture apertures corresponding to different kinds of fracture populations have been considered.

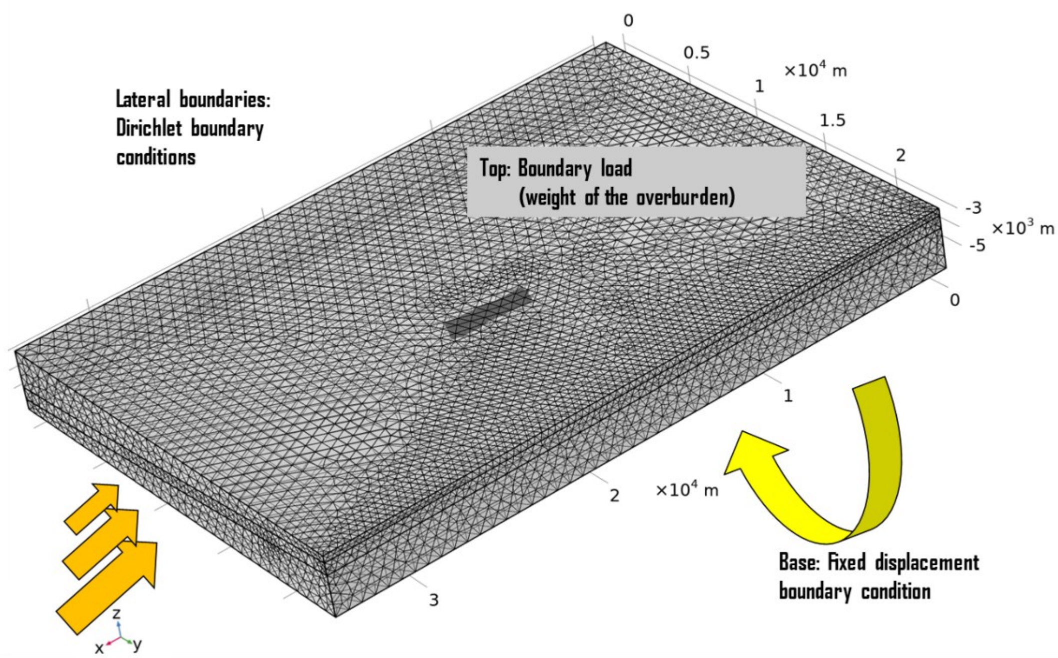

Figure 10: Adopted initial and boundary conditions for the geomechanical model to implement the assumed strike-slip stress regime and estimated principal stresses in the reservoir section. The Gartenberg fault and fracture system is located in the center of the modelling domain, which has been extended to the dimensions of ca. 24.2 km x 34.7 km x 3.2 km, while considering the down-dipping Upper Jurassic carbonates. Vertically varying size of orange arrows indicate the prescribed vertically increasing with depth displacement considered at all lateral boundaries - although different for the respective lateral boundary. Note that the y-axis denotes the North direction.

5. SIMULATION RESULTS

The finite-element software COMSOL Multiphysics® has been used in this study to numerically simulate the fully coupled thermo-hydro-mechanical reservoir processes. The study of the thermoporoelastic response of the reservoir resulting from numerous theoretical injection and production profiles envisaged in the ZoKrateS project is of great interest. In particular, we show the long-term reservoir performance resulting from 20 l/s fluid circulation as end-member scenario since this geothermal doublet exploitation scheme represent the maximum loading planned to the matrix-fracture system. To examine the overall reservoir performance affected by possible doublet operational strategies, we incorporate a second fictitious well 500 m apart at depth from the sidetrack GEN-1ST-A1, also crossing the Gartenberg fault system in accordance with the exploration concept. We carry out a variety of fully coupled thermo-hydro-mechanical model simulations focused on reservoir behavior. In this section, we show some preliminary results of a series of numerical experiments.

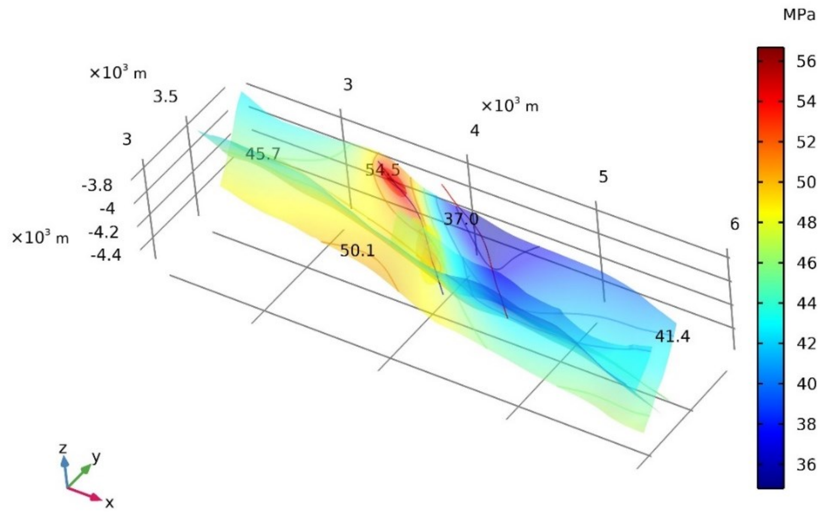

Figure 11: Pore pressure distribution in the Gartenberg fault and fracture system after 30 years of doublet operation with 20 l/s fluid circulation. The injection and production wells are depicted in blue and red, respectively. Note that the y-axis corresponds to the North direction.

Especially in a naturally fractured reservoir, the propensity of pre-existing natural fractures and faults to become reactivated after pore pressure increase due to fluid injection is critically important for the assessment of the potential of induced seismicity. Moreover, the zone of the involved faults and fractures affected by the progressing cold plume is of concern when it comes to assess the extent of the area affected by thermal induced stresses.

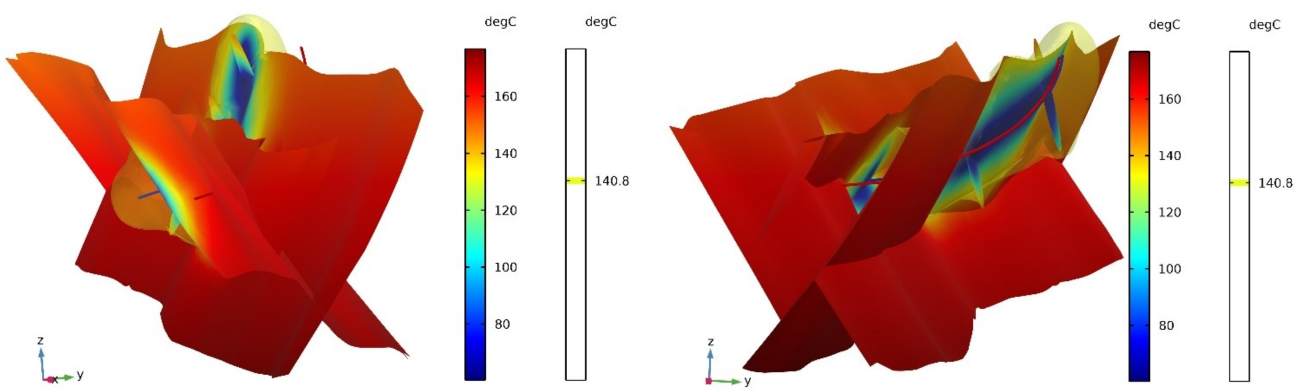

Figure 12: Temperature distribution displayed in the Gartenberg fault and fracture system after 30 years of doublet operation with 20 l/s fluid circulation. Different perspectives of the same simulation result has been displayed; from southeast (left) and northeast (right). The injection and production wells are displayed in blue and red, respectively. A 140.8 °C isotherm is shown (yellow bubble) to illustrate the cold plume extension emanating from the injector. Note that the y-axis denotes the North direction.

Fig. 11 shows the resulting pore pressure distribution after 30 years simulation time for the case of operating with a geothermal doublet scheme with constant 20 l/s injection/production rate and 60 °C injection temperature. As can be seen, a maximum pore pressure of around 56 MPa around the injection well and minimum pore pressure of ca. 35 MPa around the production well is obtained. This translates into a maximum pressure deviation from equilibrium (initial state) of 4.85 MPa. Analogously, Fig. 12 displays the temperature distribution after 30 years of geothermal doublet operation corresponding to the same thermal and hydraulic loading to the system. As illustrated by the displayed cold plume (140.8 °C isotherm), no substantial temperature drop is observed in the production well. Hence, such a scenario demonstrates the long-term reservoir performance and sustainability for a geothermal doublet configuration targeting the Gartenberg fault and fracture system. Further details concerning slip and dilation tendency analyses for the mechanical stability of the system and potentially preferential fluid flow pathways can be read in Meneses Rioseco et al. (2022).

6. CONCLUSIONS AND OUTLOOK

The project ZoKrateS has shown that the hydraulic stimulation of a deep geothermal reservoir is technically feasible with available market technology. Furthermore, the project demonstrated that it is possible to place more than approx. 330 t of proppants in the naturally fractured Upper Jurassic (Malm) carbonate reservoir without having a screen-out. In particular, seismological monitoring of these hydraulic treatments revealed no induced seismicity above background seismicity. However, key challenge remains the knowledge transfer and adoption of O&G technology to the needs and downhole conditions of geothermal projects. Especially at temperatures above 150°C, conventional completion and intervention technology reaches its design limitations.

At multiple scales, geophysical, geological and drilling operational data from the sidetrack GEN-1ST-A1 has been integrated into a structurally controlled geothermal reservoir model to define the structural and stratigraphic architecture as well as the thermal, hydraulic and mechanical parametrization of deep, low-porosity and low-permeability Upper Jurassic carbonates. For stress-sensitive fracture-controlled tight carbonates, a highly nonlinear fracture deformation was implemented to account for the normal stress dependent fracture permeability. The computational framework developed in this study is particularly efficient for the numerical simulation of coupled reservoir processes of fluid flow, heat transfer and thermoporoelastic effects that result from envisaged cold fluid injection and production schemes in fracture-dominated geothermal reservoirs. A series of numerical experiments has been conducted as to how to understand the impact that different geothermal doublet operational schemes has on the thermoporoelastic behavior and long-term sustainability of the reservoir. A second fictitious well has been inserted in the reservoir model in line with the exploration concept to perform geothermal doublet operations for future possible scenarios with optimization purposes. 3-D numerical simulations reveal the spatiotemporal evolution of pore-pressure perturbation, thermal disturbance, and resulting stress redistribution. Simulation results suggest that when considering a geothermal doublet 500 meter apart at depth, operating with 20 l/s fluid circulation and 60 °C injection temperature for the operational time envisaged, only a negligible risk to the long-term reservoir sustainability is posed. In particular, slip tendency analyses for such an end-member scenario indicate no significant mechanical instability for the Gartenberg fault and fracture system.

However, as new data is made available, further efforts are planned to implement the recently acquired data into the reservoir models developed. In particular, the permeability structure of high-density fracture networks and their hydraulic and mechanical characterization can be considered to a higher degree of resolution, as new data is reliably evaluated and interpreted. The methodology developed in this work allows to efficiently incorporate numerous scenarios and perform uncertainty analysis.

7. ACKNOWLEDGEMENTS

We are deeply indebted to the ENEX Geothermieprojekt Geretsried Nord GmbH & Co. KG for providing 3-D seismic data and data from the wellbores GEN-1 and GEN-1ST-A1. Our special thanks go also to Vladimir Shipilin for making available horizon surfaces and fault planes from the interpretation of the 3-D seismic survey in the license field Wolfratshausen. We owe sincere gratitude to the joint research project partners ENEX Geothermieprojekt Geretsried Nord GmbH & Co. KG, Geothermie Neubrandenburg GmbH (GTN), G.E.O.S. Ingenieurgesellschaft mbH and the Technical University of Munich (TUM) involved in the project Dolomitkluft for fruitful discussion. We wish to record our gratitude to Georg Stockinger for in-depth discussions and supplying recent results of his PhD-thesis covering geomechanical measurements and interpretations.

This work, within the frame of the current joint research project ZoKrateS, would not have been possible without the funding of the German Federal Ministry for Economic Affairs and Energy (BMWi) - grant number 03EE4010. The previous joint research project Dolomitkluft, from which ample data for the model parametrization has been derived, was also funded by the German Federal Ministry for Economic Affairs and Energy (grant number 0324004). We acknowledge the financial support.

REFERENCES

Bachmann, G. H. and Müller, M.: The Molasse Basin, Germany: evolution of a classic petroliferous foreland basin, in: Generation, Accumulation and Production of Europe's Hydrocarbons, edited by: Spencer, A. M., *Spec. Publ. Eur. Assoc. Petrol. Geoscien*, No. 1, 263–276, (1991), Springer-Verlag, Berlin.

Barton, N. R. & Bandis, S. C.: Characterization and modeling of the shear strength, stiffness and hydraulic behavior of rock joints for engineering purposes. In: *Rock Mechanics and Engineering, Volume 1: Principles. Editor*: X.-T. Feng, CRC Press, pp. 3-40, (2017).

Biot, M. A.: General theory of three dimensional consolidation. *Journal of Applied Physics*, 12, 155-164 (1941).

Biot, M. A.: Mechanics of deformation and acoustic propagation in porous media. *Journal of applied physics*, 33, 1482-1498 (1962).

Blank, L., Meneses Rioseco, E., Caiazzo, A. and Wilbrandt, U.: Modeling, simulation, and optimization of geothermal energy production from hot sedimentary aquifers. *Computational Geosciences*, 25, 67–104 (2021). https://doi.org/10.1007/s10596-020-09989-8.

Bourdet, D.: Well Test Analysis: The Use of Advanced Interpretation Models. Elsevier, (2002). https://doi.org/10.1017/CBO9781107415324.004.

COMSOL Multiphysics® v. 5.6: www.comsol.com. COMSOL AB, Stockholm, Sweden. 2020.

Diersch, H.-J.G.: FEFLOW. Finite Element Modeling of Flow, Mass and Heat Transport in Porous and Fractured Media. Springer Science + Business Media; Springer Heidelberg Dordrecht, London (2014). ISBN 978-3-642-387388.

Dussel, M., Moeck, I., Wolfgramm, M., Straubinger, R.: Characterization of a deep fault zone in Upper Jurassic carbonates of the Northern Alpine Foreland Basin for geothermal production (South Germany). – Proceedings 43rd Stanford Geothermal Workshop, 12.-14.02.2018, Stanford, CA (2018).

Dussel, M., Wolfgramm, M., Stockinger, G., Mraz, E., Budach, I., Moeck, I. S.: Characterisation of fault zones as geothermal targets in the deep North Alpine Foreland Basin (Southern Bavarian Molasse Basin). – Proceedings European Geothermal Congress, 11.-14. June 2019, Den Haag, the Netherlands, (2019).

Goodman, R. E.: Methods of geological engineering in discontinuous rocks. First edition, West Publishing Company, (1976).

Heat Transfer Module User's Guide, pp. 171-174.: COMSOL Multiphysics® v. 5.6. COMSOL AB, Stockholm, Sweden. 2020.

Kahnt, R., Gabriel, A., and Schlegel, M.: Verbundprojekt Dolomitkluft: Erschließung, Test und Analyse des ersten kluftdominierten Dolomitaquifers im tiefen Malm des Molassebeckens, Teilprojekt C: Abschlussbericht: Berichtszeitraum: 01.07.2016-31.12.2019. G.E.O.S. Ingenieurgesellschaft mbH, (2019). https://doi.org/10.2314/KXP:1677500433.

McTigue, D. F.: Thermoelastic response of fluid-saturated porous rock. *Journal of Geophysical Research*: Solid Earth, 91, B9, 9533-9542 (1986).

Meneses Rioseco, E., Dussel, M. and Moeck, I. S.: 3-D thermo-hydro-mechanical simulation of the behavior of a naturally fractured petrothermal reservoir in deep Upper Jurassic carbonates of the Bavarian Molasse Basin – Case Study Geretsried. *Geomechanics and Tunneling*. In press, (2022). https://onlinelibrary.wiley.com/doi/10.1002/geot.202100083.

Moeck, I., Dussel, M., Buness, H., and Wawerzinek, B.: Verbundprojekt Dolomitkluft - Erschließung, Test und Analyse des ersten kluftdominierten Dolomitaquifers im tiefen Malm des Molassebeckens; Teilprojekt E: Spannungsfeldanalyse und Charakterisierung der Störungs- und Kluftzonen: Endbericht: Laufzeit des Vorhabens: 01.05.2016-31.01.2019. Leibniz-Institut für Angewandte Geophysik Hannover, (2019). https://doi.org/10.2314/KXP:1689132620.

Reinecker, J., Tingay, M., Müller, B. and Heidbach, O.: Present-day stress orientation in the Molasse Basin. *Tectonophysics*, 482(1–4):129–38, (2010). doi:10.1016/j.tecto.2009.07.021.

Rice, J. R. and Cleary, M. P.: Some basic stress diffusion solutions for fluid saturated elastic porous media with compressible constituents. *Reviews of Geophysics and Space Physics*, 14, 227-291 (1976).

Schlumberger: Daldrup & Söhne AG – GEN-1ST-A1 6'': 4480-5287 MD - Combined Interpretation reports for FMI-HD, Sonic-HD, Fracture Ready, (2021), unpublished.

Shipilin, V., Tanner, D. C., von Hartmann, H., and Moeck, I.: Multiphase, decoupled faulting in the southern German Molasse Basin – evidence from 3-D seismic data, *Solid Earth*, 11, 2097–2117 (2020), https://doi.org/10.5194/se-11-2097-2020, 2020.

Stockinger, G. (2021) Fracturing in deep boreholes – Stress-, Structural-, & Lithology-controlled Fracture Initiation and Propagation in Deep Geothermal Boreholes in the Upper Jurassic Carbonate Rocks of the North Alpine Foreland Basin. Ph. D. Thesis, Technische Universität München (in press).

Straubinger, R. and Gahr, A.: Verbundprojekt Dolomitkluft: Erschließung, Test und Analyse des ersten kluftdominierten Dolomitaquifers im tiefen Malm des Molassebeckens, Teilprojekt A: Technische Absicherung und Öffentlichkeitsarbeit : Sachbericht (entspricht Schlussbericht nach Nr. 8.2 NKBF 98), (2018). [Enex Geothermieprojekt Geretsried Nord GmbH & Co. KG]. https://doi.org/10.2314/GBV:102353603X.

Structural Mechanics Module User's Guide.: COMSOL Multiphysics® v. 5.6. COMSOL AB, Stockholm, Sweden. 2020.

Thuro, K., Zosseder, K., Bohnsack, D., Heine, F., Konrad, F., Mraz, E., & Stockinger, G.: Abschlussbericht zu den Arbeitspaketen der Technischen Universität München zum Verbundprojekt: Dolomitkluft - Erschließung, Test und Analyse des ersten kluftdominierten Dolomitaquifers im tiefen Malm des Molassebeckens zur Erhöhung der Erfolgsaussichten : Teilprojekt B: Geomechanische und hydro-geologische Parametrisierung und Modellierung, (2019). Technische Universität München - Ingenieurfakultät Bau Geo Umwelt - Lehrstuhl für Ingenieurgeologie.

Wagner W, Kretzschmar H-J. International steam tables. Properties of water and steam based on the industrial formulation IAPWS-IF97. 2nd ed. Berlin: Springer; 2008.

Wang, H. F.: Theory of linear poroelasticity with applications to geomechanics and hydrogeology. Princeton Series in Geophysics. Princeton University Press, Princeton (2000).

Witherspoon, P. A., Wang, J. S. Y., Iwai, K. & Gale, J. E.: Validity of cubic law for fluid flow in a deformable rock fracture. *Water resources research*, Vol. 16, Issue 6, pp. 1016-1024, (1980).

Wolfgramm, M., Thiem, S., Zimmermann, J., Budach, I., Buse, C., & Kabus, F.: Erschließung, Test und Analyse des ersten kluftdominierten Dolomitaquifers im tiefen Malm des Molassebeckens: Dolomitkluft: Forschungsbericht, (2019). GTN. https://doi.org/10.2314/KXP:1670726762.

Ziegler, M. O., Heidbach, O., Reinecker, J., Przybycin, A. M., and Scheck-Wenderoth, M.: A multi-stage 3-D stress field modelling approach exemplified in the Bavarian Molasse Basin. *Solid Earth*, 7, 1365-1382, (2016). doi:10.5194/se-7-1365-2016.